Neuro-Oncology Advances

4(1), 1–13, 2022 | https://doi.org/10.1093/noajnl/vdac140 | Advance Access date 31 August 2022

T cell receptor dynamic and transcriptional determinants of T cell expansion in glioma-infiltrating T cells

Kevin Hai-Ning Lu, Julius Michel, Michael Kilian, Katrin Aslan, Hao Qi, Niklas Kehl, Stefanie Jung, Khwab Sanghvi, Katharina Lindner, Xin-Wen Zhang, Edward W Green, Isabel Poschke, Miriam Ratliff, Theresa Bunse, Felix Sahm, Andreas von Deimling, Wolfgang Wick, Michael Platten, and Lukas Bunse

DKTK Clinical Cooperation Unit (CCU) Neuroimmunology and Brain Tumor Immunology, German Cancer Research Center (DKFZ), Heidelberg, Germany (K.H.-N.L., J.M., M.K., K.A., H.Q., N.K., S.J., K.S., K.L., X.-W.Z., E.W.G., T.B., M.P., L.B.); Department of Neurology, MCTN, Medical Faculty Mannheim, Heidelberg University, Mannheim, Germany (K.H.-N.L., J.M., M.K., K.A., H.Q., N.K., S.J., K.S., X.-W.Z, E.W.G., T.B., M.P., L.B.); Department of Pediatric Hematology and Oncology, Clinic of Pediatrics III, University Hospital Essen, Essen, Germany (K.H.-N.L., K.L.); Faculty of Biosciences, University Heidelberg, Heidelberg, Germany (K.L., K.S.); Immune Monitoring Unit, National Center for Tumor Diseases (NCT), Heidelberg, Germany (K.L., I.P., M.P.); Department of Neurosurgery, University Hospital Mannheim, Mannheim, Germany (M.R.); Department of Neuropathology, Heidelberg University Medical Center, Heidelberg, Germany (F.S., A.V.D.); Department of Neurology, University Clinic Heidelberg, Heidelberg University, Heidelberg, Germany (W.W.); DKTK CCU Neurooncology, German Cancer Research Center (DKFZ), Heidelberg, Germany (W.W.); Helmholtz Institute of Translational Oncology (HI-TRON), Mainz, Germany (M.P.); DKFZ Hector Cancer Institute at the University Medical Center Mannheim, Mannheim Germany (M.P.); Medical Oncology and Internal Medicine VI, National Center for Tumor Diseases (NCT), University Hospital Heidelberg, 69120 Heidelberg, Germany (X.W.Z.); DKTK CCU Neuropathology, German Cancer Research Center (DKFZ), Heidelberg, Germany (F.S, A.V.D.); Present address: Immatics Biotechnologies GmbH, Tübingen, Germany (K.A.)

Corresponding Authors: Lukas Bunse, MD, PhD, DKTK Clinical Cooperation Unit (CCU) Neuroimmunology and Brain Tumor Immunology, German Cancer Research Center (DKFZ), Heidelberg, Germany (l.bunse@dkfz.de).

Abstract

Background. Glioblastoma (GBM) is characterized by low numbers of glioma-infiltrating lymphocytes (GIL) with a dysfunctional phenotype. Whether this dysfunctional phenotype is fixed or can be reversed upon *ex vivo* culturing is poorly understood. The aim of this study was to assess T cell receptor (TCR)-dynamics and -specificities as well as determinants of *in vitro* GIL expansion by sequencing-based technologies and functional assays to explore the use of GIL for cell therapy.

Methods. By means of flow cytometry, T cell functionality in GIL cultures was assessed from 9 GBM patients. TCR beta sequencing (TCRB-seq) was used for TCR repertoire profiling before and after *in vitro* expansion. Microarrays or RNA sequencing (RNA-seq) were performed from 6 micro-dissected GBM tissues and healthy brain RNA to assess the individual expression of GBM-associated antigens (GAA). GIL reactivity against *in silico* predicted tumor-associated antigens (TAA) and patient-individual GAA was assessed by ELISpot assay. Combined *ex vivo* single cell (sc)TCR-/RNA-seq and post-expansion TCRB-seq were used to evaluate transcriptional signatures that determine GIL expansion.

Results. Human GIL regains cellular fitness upon *in vitro* expansion. Profound TCR dynamics were observed during *in vitro* expansion and only in one of six GIL cultures, reactivity against GAA was observed. Paired *ex vivo* scTCR/RNA-seq and TCRB-seq revealed predictive transcriptional signatures that determine GIL expansion.

Conclusions. Profound TCR repertoire dynamics occur during GIL expansion. *Ex vivo* transcriptional T cell states determine expansion capacity in gliomas. Our observation has important implications for the use of GIL for cell therapy including genetic manipulation to maintain both antigen specificity and expansion capacity.

Key Points

- Glioma-infiltrating T cells regain fitness in GIL cultures.
- Expansion of glioma-infiltrating T cells is associated with profound TCR dynamics.
- ScTCR/RNA-seq reveals transcriptional signatures that determine GIL expansion.

Importance of the Study

Feasibility of glioma-infiltrating lymphocyte (GIL) therapy (GIL-T) has been demonstrated, but evidence of efficacy remains controversially discussed in the field of neuro-oncology. By means of paired *ex vivo* scTCR/RNA-seq and post-expansion TCRB-seq we find predictive transcriptional signatures that determine GIL expansion and limited functional reactivity against predefined patient-individual GBM-associated antigens (GAA). Our observation has important implications for the design of efficacious GIL-T including genetic manipulation of specific GIL subtypes to maintain both antigen specificity and expansion capacity of GIL-T products.

Malignant gliomas are the most common primary brain tumors. Despite standard of care (SOC) treatment consisting of maximal safe resection and radiochemotherapy with alkylating chemotherapy, patients with WHO grade 4 glioblastoma (GBM) still suffer from poor prognosis.[1] In recent years, cancer immunotherapy has shown promising results, especially in solid tumors with a high mutational load such as melanoma. Conversely, gliomas are tumors with low mutational load providing only very few targetable shared neoepitopes.[2–8] The majority of neoepitopes are private and subclonal with only circumstantial evidence of relevant endogenous antigen presentation.[9–12] Unspecific unleashing of exhausted particularly neoepitope-specific T cells by checkpoint inhibition even in patients with moderate temozolomide-associated hypermutation has not been efficacious.[11,13,14] However, GBM-associated antigens (GAA) derived from overexpressed genes have been identified to be naturally processed and presented in various studies assessing the human leukocyte antigen (HLA) ligandomes of gliomas including GBM.[9,15–17]

Target agnostic autologous glioma-infiltrating lymphocyte (GIL) therapy (GIL-T) circumvents time-consuming technological challenges associated with neoepitope and GAA identification and validation. Tumor-infiltrating leukocyte (TIL) therapy for primary and secondary brain tumors has not only demonstrated to be feasible,[18–21] but is considered safe as patient-derived TIL has been already subjected to central tolerance mechanisms prior to re-infusion. On the other side of the coin, quality measures of TIL products are predominantly of procedural nature as evaluation of cytotoxic capacity is time-dependent and patient-individual.

Liu *et al*. have assessed GIL phenotypes and cytokine production after *in vitro* expansion using IL-2/IL-15/IL-21, allogeneic feeder cells, and OKT3 by flow cytometry. With their expansion protocol, both $CD4^+$ and $CD8^+$ GIL predominantly exhibited a central (CCR7+ CD45RA–) and effector (CCR7– CD45RA–) memory T cell phenotype.[22] Relevant cytotoxicity was observed in all 16 established GIL cultures, but only in high effector:Target ratios, which are, in general, even in a locoregional (intraventricular, intracavitary, or intratumoral) GBM treatment regime, difficult to reach. In addition, it remains unknown, if killing is confounded by heavily pre-activated bystander T cells in distinct cell states, as the authors find cytokine-producing GILs against one predefined neoepitope (EGFRvIII) and 2 predefined GAA (survivin and NY-ESO-1) in only 0%–0.5% (median) of $CD4^+$ or $CD8^+$ GILs. In another study on TIL therapy in ovarian cancer,[23] utility of a CD137 (4-1BB)-positive separation methodology was demonstrated, but Liu *et al*. only observed limited CD137 surface expression in GIL. Importantly, GIL that showed low or absent IFN-γ production exhibited strong cytolytic reactivity in the Cr51 release assay supporting the necessity of a multifaceted understanding of GIL-T product specificities and reactivities.

Recent technological advances in transcriptional and immune receptor single cell immune profiling enable an unprecedented opportunity to monitor TCR repertoire dynamics and molecularly defined T cell states that determine the *in vitro* expansion capacity and reactivity of GILs. In combination with targeted functional testing of GIL cultures and paired *ex vivo* scTCR/RNA-seq and post-expansion TCRB-seq we aim at providing a multifaceted understanding of factors that determine GIL expansion and its implication on GIL product specificity. The knowledge of expansive factors may direct future GIL-T developments including targeted genetic manipulation to improve GIL-T products.

Materials and Methods

Patients and Sample Preparation

This study was approved by the ethics review boards of the University of Heidelberg (2018-614N-MA, 2017-589N-MA, and 2019-643N). Glioma patients (Supplementary Table 1) were diagnosed at the Institute of Neuropathology, University Hospital Heidelberg. Newly diagnosed glioma tissue and blood samples were obtained after signed informed consent. The samples were obtained in a human T cell medium (RPMI-1640 with 10% human serum, 100U ml^{-1} penicillin, 100 µg ml^{-1} streptomycin, 2 mM L-glutamine und 1.25 µg ml^{-1} fungizone) and processed immediately after surgery. Necrotic areas and vessels were removed. The remaining tumor samples were processed by mechanical dissociation. 1 cm * 1 cm tissue samples were shock frozen and used later for isolation of DNA and RNA. For *in vitro* expansion ofTIL 2 mm * 2 mm tumor fragments were put into humanT cell medium (RPMI-1640 with 10% human serum, 100 U ml^{-1} penicillin, 100 µg ml^{-1} streptomycin, 2 mM L-glutamine und 1.25 µg ml^{-1} fungizone) with 1000 U ml^{-1} IL-2 and 30 ng ml^{-1} aCD3 (OKT3) (eBioscience) and cultivated for 2 weeks. 50% of the medium was replaced with fresh medium and cytokines every 2 days.

HLA Typing

Genomic DNA was isolated from patient blood and glioma tissue using the NucleoSpinTissue Kit (Macherey-Nagel) or the Maxwell® 16 LEV Blood DNA Kit (Promega). The isolated DNA was HLA-typed as described previously.[24]

Flow Cytometry

Human samples were blocked with Human TruStain FcX Fc Receptor Blocking Solution (Biolegend) and stained with respective antibodies. eFluor 780 fixable viability dye (eBioscience) was used according to the manufacturer's protocol to exclude dead cells from analysis. For intracellular staining of cytokines, cells were incubated at 37 °C with 5 mg/mL Brefeldin A (Sigma) for 4 to 6 hours. Intracellular staining was performed using eBioscience Intracellular Fixation & Permeabilization Buffer Set for cytokines or eBioscience Foxp3/Transcription Factor Staining Buffer Set for Foxp3 staining according to manufacturer's protocol. Nonfixed samples were acquired immediately, and fixed samples were acquired within 48 hours on a FACS Canto II, a BD Aria II, or a BD LSRFortessa (all BD Biosciences).

TCRB Sequencing

For analysis of the TCR repertoire, DNA was isolated from tumor tissue and expanded TIL cultures using the *NucleoSpin Tissue Kit (Macherey-Nagel).* TCRB deep sequencing was performed to detect rearranged TCRB gene sequences using the *hsTCRB Kit* (Adaptive Biotechnologies) according to the manufacturer's protocol. Prepared libraries were sequenced on an Illumina MiSeq by the *Genomics & Proteomics Core Facility*, German Cancer Research Center (DKFZ). Data processing (demultiplexing, trimming, and gene mapping) was done using Adaptive Biotechnologies´ proprietary platform. The data was converted and analyzed using VDJtools version 1.2.1. Treemaps for visualization of the data were generated using the treemap R-package (R version 4.0.3).

Tissue Microarray and RNA-seq

Cryopreserved tumor pieces were homogenized mechanically and total RNA was isolated using the RNeasy mini kit (Qiagen) or the Maxwell 16 LEV simply RNA tissue Kit (Promega). The RNA quality was controlled for using the Nanodrop ND-1000 (ThermoFisher Scientific) and the 2100 Bioanalyzer (Agilent). As the reference to healthy tissue, pooled cDNA from 5 healthy donors (Biocat) was used. The microarray analysis was carried out using the GeneChip™ Human Genome U133 Plus 2.0 Array (Applied Biosystems™). Microarray scanning was done using an iScan array scanner. Data extraction was done for all beads individually, and outliers were removed when the absolute difference to the median was greater than 2.5 times MAD (2.5 Hampel's method). All remaining bead level data points were then quantile normalized. As a test for significance, the student's *t*-test was used on the bead expression values of the 2 groups of interest. In case of (I) significance of expression against background we tested for greater than all negative beads for this sample, in case (II) separate groups were compared, we tested for inequality of the means of the groups. In both (I) and (II) Benjamini-Hochberg correction was applied to the complete set of *P*-values of all ProbeIDs on the chip. The average expression value was calculated as the mean of the measured expressions of beads together with the standard deviation of the beads.

RNA sequencing was performed on an Illumina HiSeq4000. Raw FastQ files were mapped to the hg19 reference genome using STAR aligner version 2.7.5b followed by featureCounts version 1.6.4. For figures, Transcripts Per Million (TPM) values were compared.

Creation of Personalized Panels of Candidate Epitopes

Using microarray (n = 3) or RNA-seq data (n = 3) generated from glioblastoma patients (total n = 6) in comparison to pooled healthy brain cDNA, a personalized panel of overexpressed candidate antigens were defined for each patient. Each patient was HLA-typed to allow HLA-matched evaluation of epitopes.

I. A list of publicly available tumor-associated antigens (TAA) was extracted from *CTdatabase (n = 276)*.[25] Top 30 overexpressed TAA for each patient were defined based on gene expression results. Existing literature was browsed for reported epitopes according to the patient's HLA type. In cases where no matching epitopes could be sought out (n = 2), the top 10 overexpressed TAA were instead used for HLA-matching *in silico* prediction of epitopes using the

IEDB Processing tool as described previously.[26] In short, a total score predicting proteasomal processing, *Transporter associated with antigen processing* (TAP) transport, and MHC binding were generated for potential 9-mer and 10-mer peptides. Finally, top 5 predicted epitopes were chosen for each patient.

II. Individual glioblastoma-associated antigens (GAA) were assessed based on individual gene overexpression without prior preselection. Candidate genes showing expression above cutoff (microarray: >200 relative gene expression; RNA-seq: > 0,5 TPM) in the healthy control tissue were excluded. Noncoding RNA and inconclusive results with one probe representing multiple genes were also excluded. Top 10 overexpressed GAA were used for *in silico* epitope prediction using the IEDB Processing tool as described above and top 5 predicted epitopes were chosen for each patient.

All tested epitopes were ordered as peptides with *GenScript.*

ELISpot Assay

ELISpot white bottom multiwell plates (MAIPSWU10, Millipore) were coated with IFN-γ antibodies (1D1K) under sterile conditions and incubated at 4°C overnight. Plates were then blocked with TIL-medium (RPMI1640 with 10% FBS, 100 U ml^{-1} Penicillin, and 100 µg ml^{-1} Streptomycin) for 3 hours. TIL were seeded in a concentration of $1*10^5$ cells per well and stimulated with peptide at a concentration of 10 µg ml^{-1}. As a positive control, cells were stimulated with 20 ng ml^{-1} Phorbol-12-myristate-13-acetate (PMA) and 1 µg ml^{-1} Ionomycin. Mouse myelin oligodendrocyte glycoprotein (MOG) p35–55 MEVGWYRSPFSRVVHLYRNGK was chosen as a negative control peptide for *ex vivo* and *in vitro* stimulation. ELISpot plates were then placed in a 37°C CO_2 incubator. After 36 hours, cells were removed and IFN-γ was bound through a biotinylated IFN-γ-antibody (7-B6-1) and streptavidin-ALP, allowing visualization of spots using the *ALP conjugate substrate kit* (Bio-Rad). Spot counts were quantified using the *ImmunoSpot Analyzer* (Cellular Technology Ltd).

FACS Sorting for Single Cell RNA-Seq

Human brain tumor samples were chopped into small pieces and meshed through a 100 µm and 70 µm strainer to obtain a single cell suspension. Myelin was removed using Myelin removal beads II (Miltenyi Biotec). Human samples were frozen in 90% FBS/10% DMSO and thawed on the day of analysis.

An Aria Fusion (BD Biosciences) with the following lasers was used for cell sorting: 355, 405 nm; 488 nm; 561 nm; and 640 nm. Dissociated brain tumor samples were stained using a cocktail of the following antibodies: anti-CD3-BV510 (clone HIT3A), anti-CD45 APC-H7 (Clone 2D1), anti-CD8-FITC (clone SK1), anti-CD11b-PE/Dazzle (clone ICRF44). Fixable viability dye eFluor780 (Thermo Fisher) was used for the exclusion of dead cells. Unbiased mRNA profiling coupled with feature barcoding technology for cell surface protein (TotalSeq-C) of the sorted cells was then performed by using the chromium single cell 5′ TCR/RNA sequencing kit (10x Genomics).

Single Cell Sequencing Analysis

Single-cell RNA data were mapped to the GRChg38 reference genome using the CellRanger pipeline version 6.0 with all default settings. We excluded cells with unique feature counts over 2,500 or less than 200 as well as cells with >10% mitochondrial counts for downstream analysis. Gene expression was normalized using Seurat's LogNormalisation() and FindVariableFeatures() generated 2000 variable features. Subsequently, VDJ data were added using the combineExpression() from scRepertoireV.1.3.1. by using the amino acid sequence (CTaa) for clonotype calling. Any cell barcode with no value for the TCR beta chain was removed for further analysis. For downstream clustering TCR variable genes as well as batch effect associated features

(JUN|FOS|RP|ZFP36|EGR|HSP|MALAT1|XIST|MT|HIST|TRAV|TRAD|TRAJ|TRBV|TRBD|TRBJ|TRGV|TRGD|TRGJ|TRDV|TRDD|TRDJ)

were filtered out from the ScaleData function. The 3 patient datasets were integrated using the RunHarmony() of the harmony package version V.0.1.0 with the following parameters: max.iter.harmony = 8, max.iter.cluster = 30, dims.use = 1:30, epsilon.cluster = –Inf, epsilon.harmony = –Inf. The clustering was done using Seurat's RunUMAP(), FindNeighbours(), and FindClusters() by using 20 harmonies Dims and a resolution of 0.5. For determination of the cluster identity differential gene expression analysis was performed using MAST. In order to determine expanded TILs, TCR beta chain frequencies for each patient were compared to the matching TCR beta deep sequencing after the expansion protocol. The Top33 percent expanded TILs were used for visualization. Volcanoplots and Violinplots were generated using Seurat's FindMarkers() by again filtering out TCR variable genes as well as batch effect associated features (JUN|FOS|RP|ZFP36|EGR|HSP|MALAT1|XIST|MT|HIST|TRAV|TRAD|TRAJ|TRBV|TRBD|TRBJ|TRGV|TRGD|TRGJ|TRDV|TRDD|TRDJ) and the EnhancedVolcano package with cutoffs for Log2 fold change = 1 and *P*-value = 10e-50.

Gene ontology enrichment analysis for genes overexpressed was performed using Metascape.[27]

Statistics

Data are represented as individual values or as mean ± SEM. Group sizes (*n*) and applied statistical tests are indicated in each figure legend. Significance was assessed by either paired or unpaired *t*-test analysis or one-way ANOVA with Tukey test for multiple comparisons indicated in figure legends. Statistics were calculated using GraphPad Prism 9.0.

Data Availability

TCRB sequencing data that support the findings of this study are deposited here: https://clients.adaptivebiotech.com.

All other data and cell lines will be provided by the corresponding author upon reasonable request.

Results

Phenotypic Dynamics in GIL Cultures

Longitudinal assessment of CD3⁺ T cell frequencies in GIL cultures from newly diagnosed GBM by flow cytometry revealed a measurable relative increase of T cells starting between day 3 and 5 that was not further increased after day 12, defining our timepoint of phenotypic and sequencing-based assessment of GIL cultures at day 14 (Supplementary Figure 1A). Relative expansion of CD4⁺ GILs was higher compared to CD8⁺ GILs using an interleukin (IL)-2- and OKT3-based expansion protocol (Supplementary Figure 1B). In GIL, median expression of cluster of differentiation (CD)25, CD127, and programmed cell death protein 1 (PD-1) is highest among the canonical checkpoint molecules (CD25, CD127, CD137, CTLA-4, LAG-3, PD-1, and TIM-3).[22] Particularly PD-1 expression not only signifies an exhaustive T cell state in GIL, but has been reported as surface protein to mark tumor-reactive TIL in solid tumors.[28] In line with previous reports,[22] at day 14, the overall frequency of PD-1⁺T cells was higher in the CD4⁺ compared to the CD8⁺T cell subpopulations (Figure 1A). Interestingly, during *in vitro* expansion, CD8⁺ T cells, but not CD4⁺ T cells showed downregulation of PD-1 that was associated with proliferation and effector cytokine production of both *a priori* PD-1⁺ and PD-1– CD8⁺ T cells as assessed by granzyme B (GrzB) and Ki67 flow cytometry (Figure 1B).

T cell receptor dynamics in GIL cultures

Phenotypic alterations upon *in vitro* GIL expansion are patient-individual and expansion-protocol dependent. To assess TCR repertoire dynamics on a global scale we performed TCR beta deep sequencing (TCRB-seq) of 5 microdissected GBM patient tissues (Supplementary Table 1) *ex vivo* and post-expansion, respectively (Figure 2A–D).

Analysis showed that clonality increased sharply during expansion, indicating differential expansive capacities of T cell clonotypes (Figure 2A–C). As such, Top 10 TCR clonotypes making up 14.8% of the *ex vivo* TIL repertoire dominated the repertoire after expansion, rising to make up 61.3% of all TCR clonotypes (Figure 2A, B). Simpson diversity metrics were similar in CD4⁺ and CD8⁺T cells, suggestive for the co-occurrence of major histocompatibility complex (MHC) class I- and MHC class II-restricted T cell expansion (Figure 2C).

As indicated by color-coded treemap visualization, top 20 TCR clonotypes before and after expansion, respectively, showed no relevant overlap (Figure 2D). Most of the top frequent TCR clonotypes in the tumor *ex vivo* either expanded poorly or were lost or below TCRB-seq detection limit following *in vitro* expansion. Conversely, top frequent TCR clonotypes after *in vitro* expansion were, if at all, detected at very low frequencies in *ex vivo* TCR repertoires, indicating a strong expansion of previously nondominant T cell clonotypes.

Conceptually, GIL TCR repertoires are shaped by 2 factors *in vivo*, T cell infiltration and local antigen-driven T cell proliferation/expansion. We previously found in a phase 1 clinical trial investigating the safety and immunogenicity of a peptide vaccine targeting mutant IDH1 (IDH1-vac) in WHO grade 3 and 4 astrocytoma patients stable frequencies of top peripheral T cell clonotypes

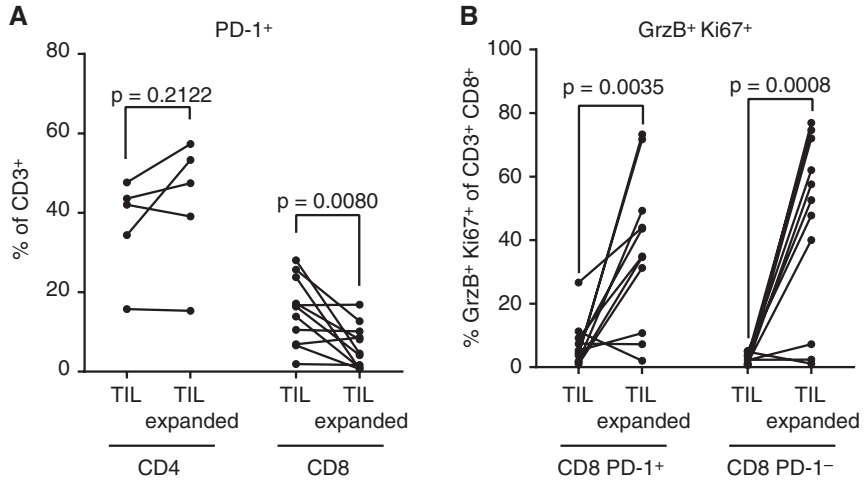

Figure 1. Phenotypic dynamics in glioma-infiltrating lymphocytes **(GIL) cultures. (A,B)**. TIL cultures isolated from GBM patients ($n = 11$) were cultured for 2 weeks and analyzed using flow cytometry. **(A)** Percentage of PD-1⁺ cells of CD4⁺ and CD8⁺ T cell subsets on days 0 and 14. **(B)** CD8⁺ TIL were sorted into PD-1⁺ and PD-1⁻ populations on day 0 and then cultured separately for 2 weeks. Percentage of GrzB⁺ Ki67⁺ CD8⁺ T cells on day 0 and day 14. **(A, B)** Statistical significance was determined by paired two-tailed *t*-tests.

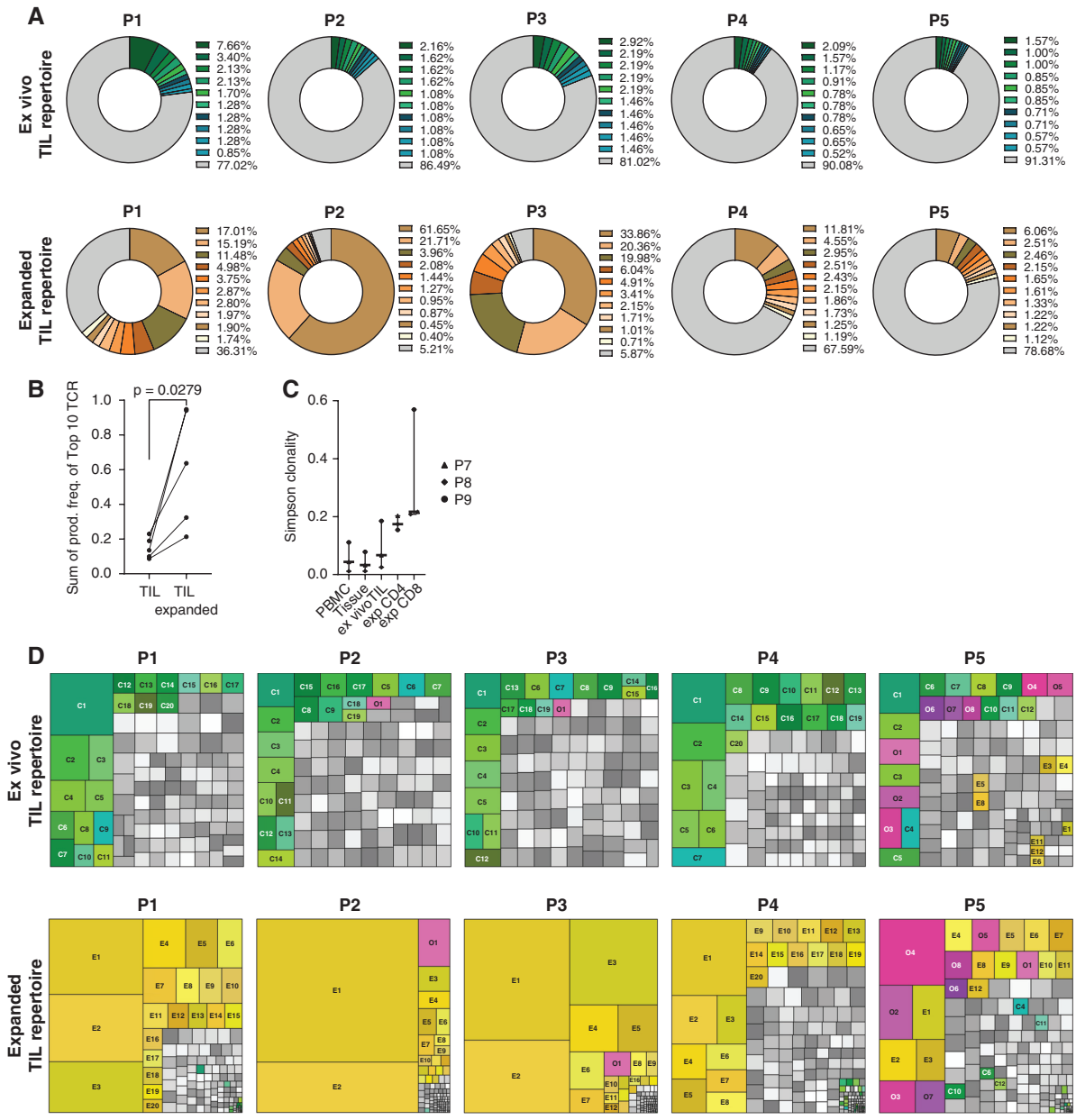

Figure 2. **T cell receptor dynamics in** glioma-infiltrating lymphocytes **(GIL) cultures. (A–D)**. TIL cultures isolated from GBM patients ($n = 5$) were cultured for 2 weeks and analyzed using TCR beta deep sequencing (TCRB-seq). **(A)** Percentage of top 10 TCR clonotypes pre- and post-expansion as a pie chart. Top 10 TCR clonotypes pre-expansion are displayed in green shades, top 10 TCR clonotypes post-expansion are displayed in yellow shades. Remaining TCR clonotypes are displayed in gray. **(B)** Quantification of (B). Sum of production frequency pre- and post-expansion. **(C)** Quantification of TCRB clonotype diversity by Simpson clonality pre- and post-expansion, as well as PBMC, CD4 GIL, and CD8 GIL. **(D)** Top 100 TCR clonotypes pre- and post-expansion as treemap. Top 20 TCR clonotypes pre-expansion displayed in green shades. Top 20 TCR clonotypes post expansion are displayed in yellow shades. TCR clonotypes featured in both top 20 lists are displayed in pink colors. **(B,C)** Statistical significance was determined by paired two-tailed t-tests.

over several weeks even in the context of a systemic immune intervention by longitudinal TCRB-sequencing of peripheral blood mononuclear cells (PBMC).[3] Hence, local antigen-driven T cell proliferation/expansion may influence to a greater extent the TCR repertoire composition. Whereas individual neoepitopes are known to be subclonal,[11] tumor-associated antigens are predominantly heterogeneous in regard to their expression level.[29] Therefore, we aimed to investigate if GIL cultures maintain their reactivity against defined tumor-associated or patient-individual GBM-associated antigens.

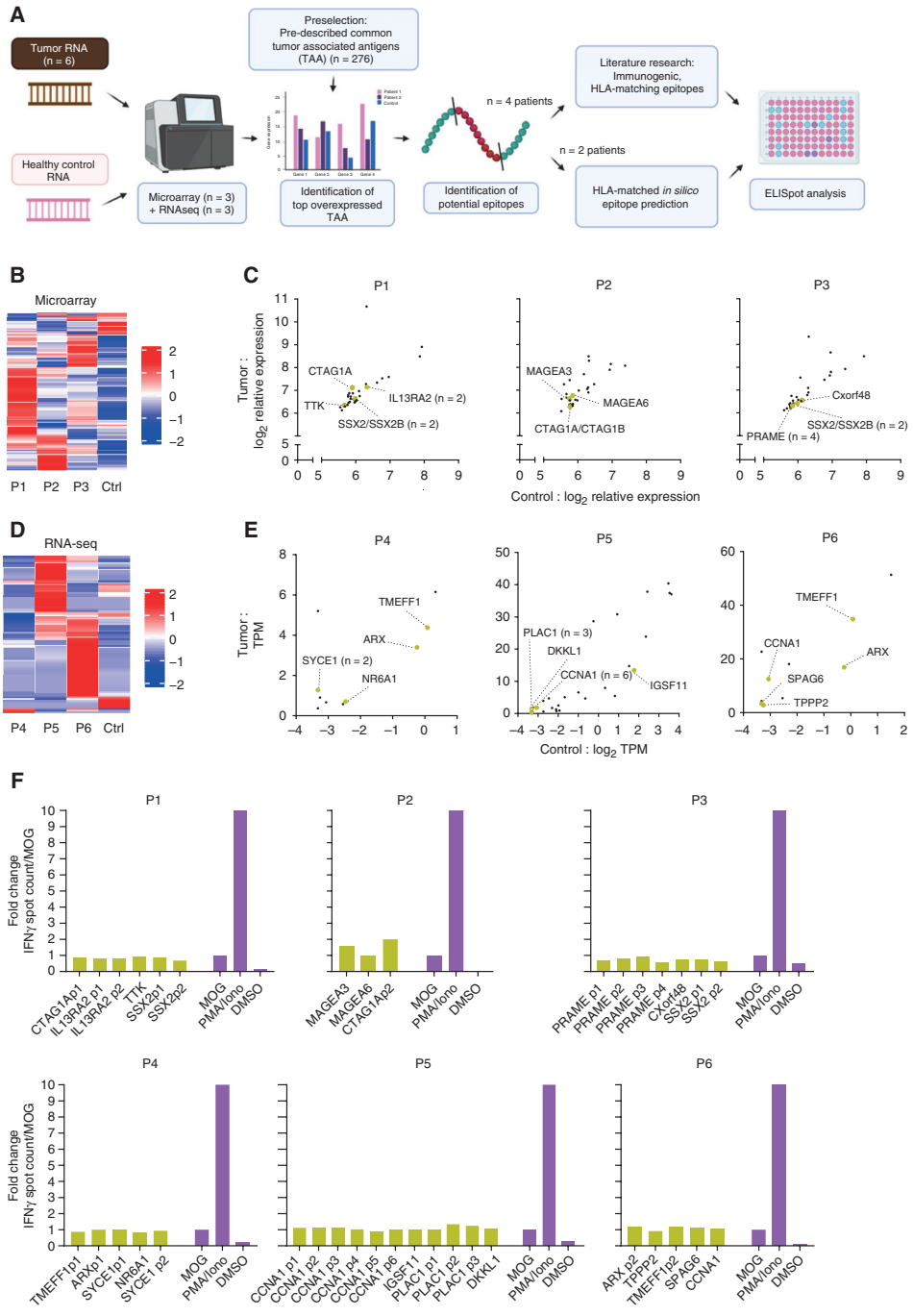

Figure 3. glioma-infiltrating lymphocytes (GIL) reactivity against common tumor-associated antigens (TAA). **(A)** Experimental overview. RNA from GBM samples ($n = 6$) and pooled healthy controls were sequenced using Microarray ($n = 3$) or RNA-seq ($n = 3$). A list of pre-described common tumor-associated antigens (TAA) were retrieved from the *CTdatabase* ($n = 276$) and ranked by patient-individualized overexpression. For Top 30 overexpressed TAA, potential epitopes were identified using literature research to retrieve pre-described, immunogenic epitopes ($n = 3$–11). For patients with rare HLA types (P4, P6), where no epitopes could be retrieved, we predicted epitopes based on the patient's HLA typing using the IEDB Processing Tool.[30] **(B–E)** Selection of overexpressed TAA candidates. **(B)** Heatmap of TAA gene expression in microarray data (P1–P3). **C)** Microarray data from $n = 3$ GBM tissues (P1–P3) compared to pooled healthy brain RNA. Top 30 overexpressed TAA genes displayed. Genes with described immunogenic, HLA-matching epitopes used for ELISpot testing are displayed in yellow. **(D)** Heatmap of TAA gene expression in RNA-seq data (P4–P6). **(E)** RNA-seq of $n = 3$ GBM tissues (P4–P6) compared to pooled healthy brain cDNA. P5: Top 30 overexpressed TAA genes displayed. Genes with described immunogenic, HLA-matching epitopes are displayed in yellow. P4, P6: Top 10 overexpressed TAA used for epitope prediction via IEDB Processing Tool displayed. Genes with the highest ranked predicted epitopes used for ELISpot testing are displayed in yellow. **(F)** ELISpot assays with autologous, expanded GIL and selected peptides (from B–E). 1×10^5 GIL were used per well. *Myelin oligodendrocyte glycoprotein* (MOG) peptide was used as the negative control.

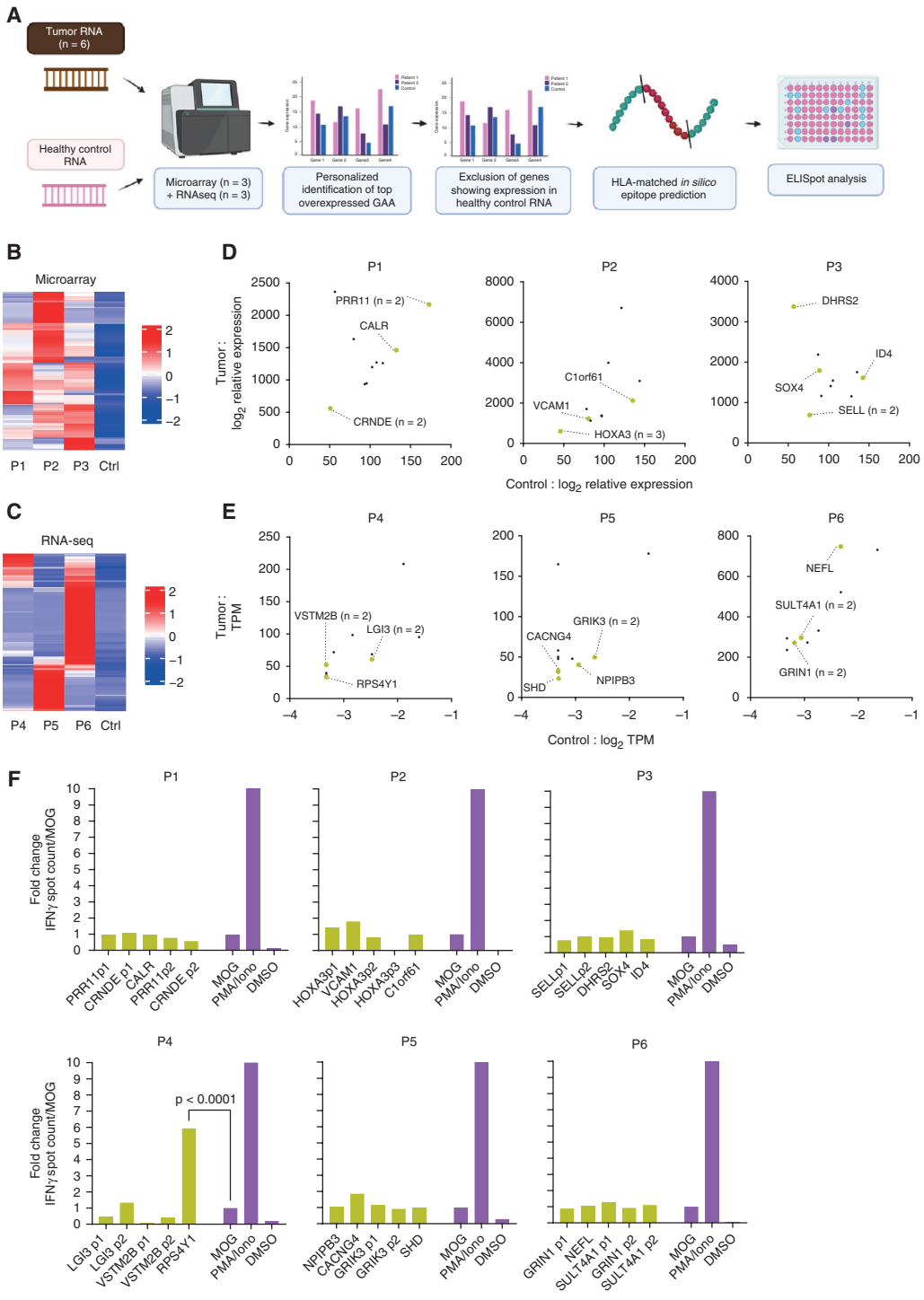

Figure 4. glioma-infiltrating lymphocytes (GIL) reactivity against patient-individual glioblastoma-associated antigens (GAA). **(A)** Experimental overview: Evaluation of GAA for ELISpot testing. Sequencing data from Figure 3. Overexpression of genes in glioblastoma patients in comparison to pooled healthy control RNA were ranked for each patient without preselection. Antigens showing expression above cutoff in the control tissue (microarray: >200 relative gene expression; RNA-seq: > 0.5 TPM) were excluded. Top 10 overexpressed genes were used for HLA-matched epitope prediction using the IEDB Processing Tool. **(B–E)** Selection of GAA candidates. **(B)** Heatmap of gene expression in microarray data (P1–P3). **C)** Heatmap of gene expression in RNA-seq data (P4–P6) **D)** Microarray data from $n = 3$ GBM tissues (P1–P3) compared to pooled healthy brain RNA. Top 10 overexpressed genes used for epitope prediction are displayed. Genes with the highest ranked predicted epitopes used for ELISpot testing are displayed in yellow. **(E)** RNA-seq of $n = 3$ GBM tissues (P4–P6) compared to pooled healthy brain RNA. Top 10 overexpressed genes used for epitope prediction are displayed. Genes with highest ranked predicted epitopes used for ELISpot testing are labelled with gene names. **(F)** ELISpot essays with autologous, expanded TIL and selected peptides (from B–E). 1×10^5 TIL were used per well. *Myelin oligodendrocyte glycoprotein* (MOG) peptide was used as the negative control. Statistical significance was determined by one-way ANOVA with the Tukey test.

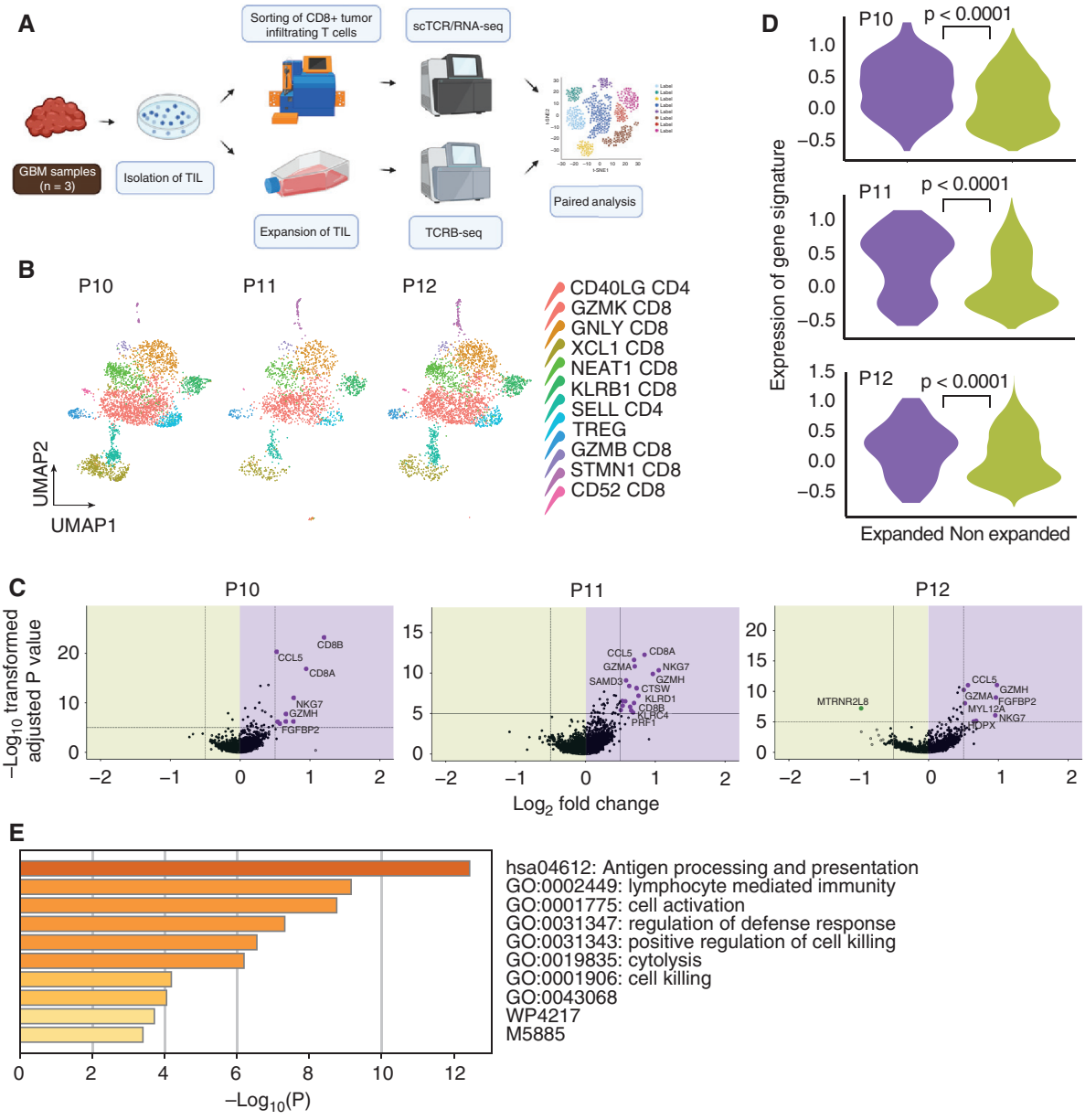

Figure 5. Transcriptional signatures determine glioma-infiltrating lymphocytes (GIL) expansion. **(A)** Experimental overview: TIL cultures isolated from *n* = 3 glioblastoma patients (P11–P12). Paired single cell (sc) TCR/RNA-seq of *ex vivo* TIL cultures (day 0) and TCRB deep sequencing of expanded TIL cultures (day 14) was performed. **(B)** Uniform Manifold Approximation and Projection (UMAP) map 8,136 cells in human high-grade gliomas (*n* = 3). Cell subsets are indicated by the color-coded legend. **(C)** Volcano plot depicting differentially expressed genes in expanded and nonexpanded TIL subsets. Highlighted genes represent top differentially expressed genes with *P*-value < .05 and average log-transformed fold change > 0.5. **(D)** Violin plots depicting the cumulative expression of the expansion-associated gene signature in expanded and nonexpanded TIL subsets. **(E)** Gene ontology analysis of the expansion-associated gene signature.

GIL Reactivity Against MHC Class I-Restricted Tumor-Associated Antigens (TAA) and Patient-Individual Glioblastoma-Associated Antigens (GAA)

To identify MHC class I-restricted tumor-associated antigens in our patient cohorts, we performed comparative expression analyses using microarray (*n* = 3) or RNA-seq (*n* = 3) of micro-dissected GBM samples and pooled healthy brain RNA (Figure 3A, Supplementary Table 1). Personalized panels of TAA and GAA were compiled based on (I) pre-described pan-cancer TAA retrieved from *CTdatabase* (*n* = 276) (Supplementary Table 2) and (II) GAA from patient-individual expression analysis, respectively. Results from gene expression analysis were used to rank potential antigens by overexpression. HLA typing was

performed for all study patients to select HLA-matching epitopes (Supplementary Table 3). Microarrays are suitable for the semiquantitative assessment of rare transcripts. Hence, we first used this array-based method for 3 GBM patient samples (P1–3) to identify the number and expression level of transcripts (TAA) that match transcripts from previously reported common TAA retrieved from *CTdatabase* (Figure 3B, C; Supplementary Table 4). Interestingly, except for a few transcripts such as SSX peptide 2 between P1 and P3 and *CTAG1A* between P1 and P2, array-based assessment of TAA expression was very heterogeneous. Some TAA transcripts were even higher expressed in reference to healthy brain RNA. Subsequently, the top 30 overexpressed TAA per patient (P1–3) were chosen and used to browse for experimentally validated immunogenic MHCI-restricted epitopes (Figure 3A). Applying this algorithm, 3 to 7 MHCI-restricted epitopes per patient were selected for the assessment of spontaneous intratumoral T cell responses (Supplementary Table 5). ELISpots were performed for each patient using GIL cultures. However, none of the selected HLA-matched TAA peptides elicited a robust IFN-γ response when incubated with the corresponding GIL culture (Figure 3F).

Next, we adopted our experimental setup using RNA-seq instead of an array-based assessment of candidate expression in 3 additional GBM patient samples (P4–P6) (Figure 3A). Indeed, compared to the array-based assessments, the range of intraindividual TAA candidate expression levels was larger (Figure 3D, E; Supplementary Table 6). Following our candidate prioritization algorithm, eleven MHCI-restricted epitopes were selected for the assessment of spontaneous intratumoral T cell responses for patient P5. For patients P4 and P6, no HLA-matching TAA candidates were found. For the latter, the top 10 overexpressed TAA were instead used for HLA-matching *in silico* prediction of epitopes using the *IEDB Processing tool*[30] (Supplementary Table 7). A total score predicting proteasomal processing, TAP transport, and MHC binding was generated for potential 9-mer and 10-mer peptides. Finally, top 5 predicted epitopes were chosen for each patient. Overlaps of predicted TAA were found for *ARX* between P4 and P6 and *CCNA1* between P5 and P6.

Similar to our array-based approach, no IFN-γ production for epitope-derived peptides was observed when incubated with the corresponding GIL culture (Figure 3F). Taken together, we were not able to provide evidence of T cell reactivity against validated actively HLA-matched TAA in 6 GIL cultures. Overall, the expression level of HLA-matched TAA was low to intermediate.

Because of these experimental observations and the difficulty of general conclusions on post-expansion GIL reactivity we next focused on top patient-individual overexpressed genes (GAA) for the same patient samples (P1–6) (Figure 4A–E). GAA (microarray (Figure 4B,D) and RNA-seq (Figure 4C,E)) were ranked based on patient-individual overexpression. Candidate transcripts showing expression above the cutoff (microarray: > 200 relative gene expression; RNA-seq: > 0.5TPM) in the healthy control tissue were excluded from our analysis (Supplementary Table 8). Top 10 ranked antigens were again selected for HLA-matched *in silico* epitope predictions using the *IEDB* processing algorithm (Figure 4D, E; Supplementary Table 9). Five *in silico* HLA-matched MHCI-restricted peptides per patient were chosen for functional testing. There was no overlap of selected GAA between patients (Figure 4F). Interestingly, patient-individual GAA did not match any of the externally validated TAA (see Figure 3). Of the selected GAA, restimulation with an RPS4Y1-derived 10-mer peptide showed a robust IFN-γ response in patient P4, defined as a fold change >5 compared to an irrelevant control peptide (Figure 4F). Importantly, the expression of RPS4Y1 was below the relevant threshold in the control tissue (TPM <0.1). The GAA-associated overexpression in patient sample P4 was 333.6-fold. The identified HLA-B*44:03-restricted 10-mer peptide had a total prediction score of 1.25.[30] Overall, in our study, n = 68 HLA-matched tumor-associated peptides were synthesized and selected based on different prioritization algorithms, but only 1 of 6 GIL cultures showed antigen-specific reactivity against 1 candidate GAA. Although this targeted approach has inevitable limitations in sensitivity, the lack of antigen-reactivity is at least suggestive of antigen-independent determinants of T cell expansion.

Transcriptional Signatures Determine GIL Expansion

To assess if transcriptional T cell signatures at the critical time point of tumor resection drive GIL expansion, we performed paired *ex vivo* single cell (sc)TCR/RNA-seq and post-expansion TCRB-seq in 3 GBM patient samples (P10–12) (Figure 5A, Supplementary Table 1). We sorted 8,136 $CD8^+$ T cells from *ex vivo* dissociated GBM patient samples (Figure 5A, Supplementary Figure 5A) and subjected them to combined scTCR/RNA-seq (Figure 5B, Supplementary Figure 5B). To define the expanding T cell clonotypes, TCRB-seq of corresponding GIL cultures was performed after *in vitro* expansion (day 14) (Figure 5A). Expanded T cell subsets were determined by comparison of relative T cell clonotype frequency *ex vivo* and post-expansion (top 33%) (Supplementary Figure 5C). Based on their expansion capacity, we grouped T cell clonotypes into an expander and nonexpander GIL-T cells. In the expander T cell population, differential gene analyses showed increased expression of several genes associated with T cell activation (Figure 5C). Of these genes, *Granzyme A* (GrzA), *Granzyme H* (GrzH), *Chemokine ligand 5* (CCL5), *Natural killer cell granule protein 7* (NKG7), and *Granulysin* (GNLY) were found to be highly expressed on expander T cells in 2 of 3 GBM patient samples. Expression analysis of this activation-associated gene signature showed robust upregulation in the expanded T cell subset of all 3 patients (Figure 5D). Gene ontology analysis showed an activated, pro-inflammatory gene signature that is involved in antigen processing and presentation as well as cell activation and cytolysis (Figure 5E). Taken together, by using multimodal and longitudinal immune receptor and transcriptome sc-RNA-seq we identified an *ex vivo* T cell transcriptional signature that correlates with GIL expansion. Further studies are required for validation in other glioma entities and beyond.

Discussion

Based on intensified collaborations between regularity authorities and academic centers worldwide, as well as

substantial technological advances including closed Good Manufacturing Practice (GMP)-compatible systems to culture and manufacture T cell products,[31] TIL therapy is becoming clinically scalable. For GBM patients, there is an obvious unmet clinical need to evaluate highly potent cellular therapies. Whereas pros and cons of various administration routes of cellular T cell products in GBM patients are intensively discussed elsewhere,[32] we aimed here at assessing TCR-specificity, TCR dynamics, and transcriptional determinants of T cell expansion in GIL cultures by means of peptide-based recall responses, paired *ex vivo* single cell (sc)TCR/RNA-seq and post-expansion TCRB-seq. Our data demonstrate that *in vitro,* both $CD4^+$ and $CD8^+$ T cells not only expand but start to produce important effector cytokines as soon as they are removed from the immunosuppressive and hypoxic microenvironment of GBM. It is tempting to speculate, that in an initial phase of GIL culture establishment, tumor-associated macrophages and/or microglia successfully acquire a pro-inflammatory phenotype in addition, restoring MHCII-restricted antigen presentation capacity orchestrating an MHCI- and MHCII-antigen directed T cell expansion.

Although multicenter phase 1 clinical trial in GBM applying personalized neoepitope-specific vaccines have demonstrated feasibility, immunogenicity, and safety, the majority of neoepitopes are predominantly MHCII-restricted, private, and subclonal in GBM. In general, only a few antigens lead to the presence of neoepitope-specific intratumoral T cell clonotypes. Conversely, tumor-associated antigens (TAA) derived from overexpressed genes have been intensively studied to be naturally processed and presented in various studies assessing HLA ligandomes of gliomas and other cancers. Frequently, these antigenic proteins harbor MHCI-restricted antigens, but it remains challenging to map a minimal epitope precisely when using sequencing-based screening algorithms. In this study, we took several strategies to probe GIL culture reactivity against selected predicted or experimentally validated TAA- or GAA-derived peptides, respectively, but only found 1 of 6 GIL cultures to specifically recognize the patient-individual MHCI-restricted 10-mer GAA antigen RPS4Y1(AEMVVEAEIF). Although we cannot exclude that some nonselected TAA are in principle recognized by our established GIL cultures, it has been reported that TAA are less likely to induce an endogenous immune response because high-affinity T cells that respond to unmutated peptides are subjected to central tolerance.[33] Hence, albeit robust T cell expansion and phenotypical cellular fitness, we found very limited evidence of a truly antigen-directed T cell expansion in our study on GIL cultures. As found in other solid tumors, 1 explanation for this finding is spatial heterogeneity[34] and GBM is explicitly known to be a highly heterogeneous disease. Therefore, we cannot exclude that spatial T cell and antigen heterogeneity has an impact on antigen-directed T cell expansion *in vitro*. As of now, efficacy of GIL therapy for glioma patients remains unclear. Quattrocci *et al*.[35] used expanded autologous TIL and although the authors were able to observe clinical responses in some glioma patients following re-infusion of cells in combination with IL-2 therapy, there was limited evidence of selective cytotoxicity. It is tempting to speculate that, in line with our observation, this is due to the lack of post-expansion antigen selectivity. Likewise, a number of other studies using the transfer of autologous cells resulted in limited signs of efficacy in brain tumors.[19,36,37] Importantly, we found recently that a molecularly defined subset of $CXCL13^+$ $CD4^+$ T cells expressed a unique IDH1-vac-induced TCR recognizing the neoantigen IDH1R132H in an astrocytoma patient receiving IDH1-vac with SOC. *CXCL13* and other transcripts including *PDCD1* (PD-1) and *TIGIT* as part of distinct gene signatures seem applicable for the selection or enrichment of truly tumor-reactive T cell clonotypes in gliomas and beyond.[38] However, the impact of these molecules for T cell *in vitro* expansion remains unknown. Here we defined a novel gene set including *Granzyme A* (GrzA), *Granzyme H* (GrzH), *Chemokine ligand 5* (CCL5), *Natural killer cell granule protein 7* (NKG7) and *Granulysin* (GNLY) that determines T cell clonotypes with expansive capacity in GIL cultures by paired *ex vivo* single cell (sc)TCR/RNA-seq and post-expansion TCRB-seq. If this gene signature defines T cell subsets with overall enhanced proliferative capacity or a distinct cell state that can more rapidly proliferate *in vitro*, needs to be further investigated. Our GIL reactivity data suggests that both proliferation and cytokine production of bystander T cells as well as, in lower frequencies, true reinvigoration of tumor-reactive T cells occurs. Moreover, it is tempting to speculate, that prior therapies and glioma genotype-dependent immune microenvironmental specificities as found in IDH-mutant gliomas,[39–44] may influence such T cell signatures.

Supplementary Material

Supplementary material is available at *Neuro-Oncology Advances* online.

Keywords

cellular immunotherapy | glioma | glioma-infiltrating lymphocytes |TCR-seq |TCR repertoire.

Funding

This study was supported by grants from the Swiss Cancer Foundation (Swiss Bridge Award), the Else Kröner Fresenius Foundation (EKMS), the University Heidelberg Foundation, the DFG (German Research Foundation) – CRC1389 – UNITE Glioblastoma B03, and the Sybille Assmuss Foundation to L.B.; The German Cancer Aid (Deutsche Krebshilfe, reference number 70114417), the DFG, project 404521405 (CRC1389 UNITE Glioblastoma B01) to T.B. and M.P., and DFG, project PL-315/9-1 (RTG2727 "Innate Immune Checkpoints in Cancer and Tissue Damage", and the DKTK Joint Funding AMI2GO to M.P.; and the Rolf Schwiete Foundation (2021-009) to L.B and M.P.

Acknowledgments

We thank the patients and their relatives for the support of this study. We acknowledge the support of the DKFZ Genomics and Proteomics Core Facility, the Flow Cytometry Core Facility and the single cell Open Lab at the German Cancer Research Center. We acknowledge the data storage service SDS@hd supported by the Ministry of Science Germany.

Conflict of Interest

E.W.G., M.P., K.L., and L.B are inventors and patent-holders on "Gene Signatures for the selection of tumor-reactive T cell receptor" (PCT/EP2022/057672). T.B., W.W., and M.P. are inventors and patent-holders on "Peptides for use in treating or diagnosing IDH1R132H positive cancers" (EP2800580B1). The other authors have no conflict of interest.

Authorship Statement.

Performed experiments and wrote the manuscript: K.H.N.L.
Performed experiments: M.K., J.M., H.Q., K.A., S.J., N.K., K.L.
Analyzed and interpreted data: E.W.G, I.P.
Provided and analyzed human tissue samples: M.R., F.S., A.v.D.
Edited manuscript, analyzed and interpreted data: T.B., W.W.
Conceptualized the study, wrote the paper, analyzed and interpreted data: M.P. and L.B.

References

1. Stupp R, Mason WP, van den Bent MJ, et al. Radiotherapy plus concomitant and adjuvant temozolomide for glioblastoma. *N Engl J Med.* 2005;352(10):987–996.
2. Kilian M, Friedrich M, Sanghvi K, et al. T-cell receptor therapy targeting mutant capicua transcriptional repressor in experimental gliomas. *Clin Cancer Res.* 2022;28(2):378–389.
3. Platten M, Bunse L, Wick A, et al. A vaccine targeting mutant IDH1 in newly diagnosed glioma. *Nature.* 2021;592:463–468.
4. Schumacher T, Bunse L, Pusch S, et al. A vaccine targeting mutant IDH1 induces antitumour immunity. *Nature.* 2014;512(7514):324–327.
5. Ochs K, Ott M, Bunse T, et al. K27M-mutant histone-3 as a novel target for glioma immunotherapy. *Oncoimmunology.* 2017;6(7):e1328340.
6. Chheda ZS, Kohanbash G, Okada K, et al. Novel and shared neoantigen derived from histone 3 variant H3.3K27M mutation for glioma T cell therapy. *J Exp Med.* 2018;215(1):141–157.
7. Pellegatta S, Valletta L, Corbetta C, et al. Effective immuno-targeting of the IDH1 mutation R132H in a murine model of intracranial glioma. *Acta Neuropathol Commun.* 2015;3:4.
8. Weller M, Butowski N, Tran DD, et al. Rindopepimut with temozolomide for patients with newly diagnosed, EGFRvIII-expressing glioblastoma (ACT IV): a randomised, double-blind, international phase 3 trial. *Lancet Oncol.* 2017;18(10):1373–1385.
9. Hilf N, Kuttruff-Coqui S, Frenzel K, et al. Actively personalized vaccination trial for newly diagnosed glioblastoma. *Nature.* 2019;565(7738):240–245.
10. Keskin DB, Anandappa AJ, Sun J, et al. Neoantigen vaccine generates intratumoral T cell responses in phase Ib glioblastoma trial. *Nature.* 2019;565(7738):234–239.
11. Touat M, Li YY, Boynton AN, et al. Mechanisms and therapeutic implications of hypermutation in gliomas. *Nature.* 2020;580(7804):517–523.
12. Valentini D, Rao M, Meng Q, et al. Identification of neoepitopes recognized by tumor-infiltrating lymphocytes (TILs) from patients with glioma. *Oncotarget.* 2018;9(28):19469–19480.
13. Omuro A, Vlahovic G, Lim M, et al. Nivolumab with or without ipilimumab in patients with recurrent glioblastoma: results from exploratory phase I cohorts of CheckMate 143. *Neuro Oncol.* 2018;20(5):674–686.
14. Reardon DA, Brandes AA, Omuro A, et al. Effect of nivolumab vs bevacizumab in patients with recurrent glioblastoma: the CheckMate 143 phase 3 randomized clinical trial. *JAMA Oncol.* 2020;6(7):1003–1010.
15. Dutoit V, Herold-Mende C, Hilf N, et al. Exploiting the glioblastoma peptidome to discover novel tumour-associated antigens for immunotherapy. *Brain.* 2012;135(Pt 4):1042–1054.
16. Migliorini D, Dutoit V, Allard M, et al. Phase I/II trial testing safety and immunogenicity of the multipeptide IMA950/poly-ICLC vaccine in newly diagnosed adult malignant astrocytoma patients. *Neuro Oncol.* 2019;21(7):923–933.
17. Shraibman B, Barnea E, Kadosh DM, et al. Identification of tumor antigens among the HLA peptidomes of glioblastoma tumors and plasma. *Mol Cell Proteomics.* 2018;17(11):2132–2145.
18. Dillman RO, Duma CM, Ellis RA, et al. Intralesional lymphokine-activated killer cells as adjuvant therapy for primary glioblastoma. *J Immunother.* 2009;32(9):914–919.
19. Dillman RO, Duma CM, Schiltz PM, et al. Intracavitary placement of autologous lymphokine-activated killer (LAK) cells after resection of recurrent glioblastoma. *J Immunother.* 2004;27(5):398–404.
20. Rosenberg SA, Packard BS, Aebersold PM, et al. Use of tumor-infiltrating lymphocytes and interleukin-2 in the immunotherapy of patients with metastatic melanoma. A preliminary report. *N Engl J Med.* 1988;319(25):1676–1680.
21. Mehta GU, Malekzadeh P, Shelton T, et al. Outcomes of adoptive cell transfer with tumor-infiltrating lymphocytes for metastatic melanoma patients with and without brain metastases. *J Immunother.* 2018;41(5):241–247.
22. Liu Z, Meng Q, Bartek J, Jr, et al. Tumor-infiltrating lymphocytes (TILs) from patients with glioma. *Oncoimmunology.* 2017;6(2):e1252894.
23. Ye Q, Song DG, Poussin M, et al. CD137 accurately identifies and enriches for naturally occurring tumor-reactive T cells in tumor. *Clin Cancer Res.* 2014;20(1):44–55.
24. Lange V, Bohme I, Hofmann J, et al. Cost-efficient high-throughput HLA typing by MiSeq amplicon sequencing. *BMC Genomics.* 2014;15:63.
25. Almeida LG, Sakabe NJ, deOliveira AR, et al. CTdatabase: a knowledge-base of high-throughput and curated data on cancer-testis antigens. *Nucleic Acids Res.* 2009;37(Database issue):D816–D819.
26. Fleri W, Paul S, Dhanda SK, et al. The immune epitope database and analysis resource in epitope discovery and synthetic vaccine design. *Front Immunol.* 2017;8:278.
27. Zhou Y, Zhou B, Pache L, et al. Metascape provides a biologist-oriented resource for the analysis of systems-level datasets. *Nat Commun.* 2019;10(1):1523.
28. Gros A, Robbins PF, Yao X, et al. PD-1 identifies the patient-specific CD8(+) tumor-reactive repertoire infiltrating human tumors. *J Clin Invest.* 2014;124(5):2246–2259.

29. Patel AP, Tirosh I, Trombetta JJ, et al. Single-cell RNA-seq highlights intratumoral heterogeneity in primary glioblastoma. *Science.* 2014;344(6190):1396–1401.
30. Vita R, Mahajan S, Overton JA, et al. The Immune Epitope Database (IEDB): 2018 update. *Nucleic Acids Res.* 2019;47(D1):D339–D343.
31. Mock U, Nickolay L, Philip B, et al. Automated manufacturing of chimeric antigen receptor T cells for adoptive immunotherapy using CliniMACS prodigy. *Cytotherapy.* 2016;18(8):1002–1011.
32. Elmadany N, Alhalabi OT, Platten M, Bunse L. Site-specific considerations on engineered T cells for malignant gliomas. *Biomedicines.* 2022;10(7):1738.
33. Mohme M, Neidert MC, Regli L, Weller M, Martin R. Immunological challenges for peptide-based immunotherapy in glioblastoma. *Cancer Treat Rev.* 2014;40(2):248–258.
34. Poschke IC, Hassel JC, Rodriguez-Ehrenfried A, et al. The outcome of ex vivo TIL expansion is highly influenced by spatial heterogeneity of the tumor T-Cell repertoire and differences in intrinsic in vitro growth capacity between T-cell clones. *Clin Cancer Res.* 2020;26(16):4289–4301.
35. Quattrocchi KB, Miller CH, Cush S, et al. Pilot study of local autologous tumor infiltrating lymphocytes for the treatment of recurrent malignant gliomas. *J Neurooncol.* 1999;45(2):141–157.
36. Jacobs SK, Wilson DJ, Kornblith PL, Grimm EA. Interleukin-2 or autologous lymphokine-activated killer cell treatment of malignant glioma: phase I trial. *Cancer Res.* 1986;46(4 Pt 2):2101–2104.
37. Hayes RL, Koslow M, Hiesiger EM, et al. Improved long term survival after intracavitary interleukin-2 and lymphokine-activated killer cells for adults with recurrent malignant glioma. *Cancer.* 1995;76(5):840–852.
38. Lowery FJ, Krishna S, Yossef R, et al. Molecular signatures of antitumor neoantigen-reactive T cells from metastatic human cancers. *Science.* 2022;375(6583):877–884.
39. Friebel E, Kapolou K, Unger S, et al. Single-cell mapping of human brain cancer reveals tumor-specific instruction of tissue-invading leukocytes. *Cell.* 2020;181(7):1626–1642.e20.
40. Bunse L, Pusch S, Bunse T, et al. Suppression of antitumor T cell immunity by the oncometabolite (R)-2-hydroxyglutarate. *Nat Med.* 2018;24(8):1192–1203.
41. Klemm F, Maas RR, Bowman RL, et al. Interrogation of the microenvironmental landscape in brain tumors reveals disease-specific alterations of immune cells. *Cell.* 2020;181(7):1643–1660.e17.
42. Amankulor NM, Kim Y, Arora S, et al. Mutant IDH1 regulates the tumor-associated immune system in gliomas. *Genes Dev.* 2017;31(8):774–786.
43. Kohanbash G, Carrera DA, Shrivastav S, et al. Isocitrate dehydrogenase mutations suppress STAT1 and CD8+ T cell accumulation in gliomas. *J Clin Invest.* 2017;127(4):1425–1437.
44. Friedrich M, Sankowski R, Bunse L, et al. Tryptophan metabolism drives dynamic immunosuppressive myeloid states in IDH-mutant gliomas. *Nat Cancer.* 2021;2(7):723–740.